Published in final edited form as:
J Bone Miner Res. 2014 July ; 29(7): 1619–1626. doi:10.1002/jbmr.2195.

High-Resolution Genome Screen for Bone Mineral Density in Heterogeneous Stock Rat

Imranul Alam[a], **Daniel L. Koller**[b], **Toni Cañete**[d], **Gloria Blázquez**[d], **Regina López-Aumatell**[c], **Esther Martínez-Membrives**[d], **Sira Díaz-Morán**[d], **Adolf Tobeña**[d], **Alberto Fernández-Teruel**[d], **Pernilla Stridh**[e], **Margarita Diez**[e], **Tomas Olsson**[e], **Martina Johannesson**[e], **Amelie Baud**[c], **Michael J. Econs**[a,b], and **Tatiana Foroud**[a,b]

[a]Medicine, Indiana University School of Medicine, IN, USA

[b]Medical and Molecular Genetics, Indiana University School of Medicine, IN, USA

[c]Wellcome Trust Center for Human Genetics, Oxford OX3 7BN, United Kingdom

[d]Department of Psychiatry and Forensic Medicine, Institute of Neurosciences, School of Medicine, Universitat Autònoma deBarcelona, 08193-Bellaterra, Barcelona, Spain

[e]Clinical Neuroscience, Center for Molecular Medicine, Neuroimmunolgy Unit, Karolinska Institutet, S171 76 Stockholm, Sweden

Abstract

We previously demonstrated that skeletal mass, structure and biomechanical properties vary considerably in heterogeneous stock (HS) rat strains. In addition, we observed strong heritability for several of these skeletal phenotypes in the HS rat model, suggesting that it represents a unique genetic resource for dissecting the complex genetics underlying bone fragility. The purpose of this study was to identify and localize genes associated with bone mineral density in HS rats. We measured bone phenotypes from 1524 adult male and female HS rats between 17 to 20 weeks of age. Phenotypes included DXA measurements for bone mineral content and areal bone mineral density for femur and lumbar spine (L3-5), and volumetric BMD measurements by CT for the midshaft and distal femur, femur neck and 5th lumbar vertebra. A total of 70,000 polymorphic SNPs distributed throughout the genome were selected from genotypes obtained from the Affymetrix rat custom SNPs array for the HS rat population. These SNPs spanned the HS rat genome with a mean linkage disequilibrium coefficient between neighboring SNPs of 0.95. Haplotypes were estimated across the entire genome for each rat using a multipoint haplotype reconstruction method, which calculates the probability of descent for each genotyped locus from each of the 8 founder HS strains. The haplotypes were tested for association with each bone density phenotype via a mixed model with covariate adjustment. We identified quantitative trait

Corresponding author: Imranul Alam, PhD Department of Medicine Indiana University School of Medicine 541 Clinical Dr, CL459 Indianapolis, IN 46202 Phone (317) 274-0744 Fax (317) 278-0658 ialam@iupui.edu.

Authors' roles

Study design: IA, DLK, MJE, and TF. Study conduct: IA, DLK, TC, GB, RL, EM, SD, AT, AF, PS, MD, TO, MJ, and AB. Data analysis: IA, DLK, AB, and TF. Data interpretation: IA, DLK, MJE and TF. Drafting manuscript: IA and DLK. Revising manuscript content: IA, DLK, AF, MJE, and TF. Approval of final version of manuscript: IA, DLK, TC, GB, RL, EM, SD, AT, AF, PS, MD, TO, MJ, AB, MJE and TF.

Conflict of Interest: All authors have no conflicts of interest.

loci (QTLs) for bone mineral density phenotypes on chromosomes 2, 9, 10 and 13 meeting a conservative genome-wide empiric significance threshold (FDR=5%; $P<3 \times 10^{-6}$). Importantly, most QTLs were localized to very small genomic regions (1-3 Mb), allowing us to identify a narrow set of potential candidate genes including both novel genes and genes previously shown to have roles in skeletal development and homeostasis.

Keywords

Heterogeneous stock rat; Bone density; Genes; Osteoporosis; Genetics

Introduction

Osteoporosis is a common bone disease leading to increased susceptibility to fracture at multiple skeletal sites[1] resulting in a substantial public health burden. Bone mineral density (BMD), structure and strength are the major determinants for skeletal fracture.[2-4] Several studies demonstrated that these phenotypes are highly heritable.[5-8] As much as 80% of the variability of BMD is due to heritable factors.[7] Identification of genes underlying BMD phenotypes, particularly at the most common skeletal fracture sites, will provide valuable insights for understanding the genetics of osteoporosis and fracture risk.

Previously, using 4 inbred rats (F344, LEW, COP and DA), we identified several chromosomal regions linked to bone density, structure and strength phenotypes.[9-13] Although, these inbred rat models have served an important role in genetic mapping for bone fragility phenotypes, most of these QTLs encompass 20 to 30 cM and harbor hundreds of potential candidate genes. Subsequently, using genomic expression analysis, we identified several potential candidate genes within some of these QTLs.[14-16] However, it is a formidable challenge to narrow these critical QTL regions to a small chromosomal segment containing a few genes. Several alternative approaches such as the development of recombinant inbred and congenic lines have been attempted, but these approaches have proven to be time-consuming and labor intensive and often do not have enough resolution to detect the causal genes and variants, especially those of relatively small effect.

The heterogeneous stock (HS) rat, a unique rat model, was developed by the National Institutes of Health (NIH) in 1984.[17] These rats were originally derived from eight inbred founder strains: Agouti (ACI/N), Brown Norway (BN/SsN), Buffalo (BUF/N), Fischer 344 (F344/N), M520/N, Maudsley Reactive (MR/N), Wistar-Kyoto (WKY/N) and Wistar-Nettleship (WN/N).[17] Subsequently, this stock was bred for 50 generations using a rotational outbreeding regime to minimize the extent of inbreeding, drift and fixation.[18] Importantly, each of these HS rats represents a unique, genetically random mosaic of founding animal chromosomes due to recombination that have accumulated over many generations. It has been estimated that the average distance between recombination events in these rats is approximately 2 cM.[19] Thus, the HS rat is a unique genetic resource for the fine mapping of QTLs to very small genomic regions. Recently, these rats have been successfully used to fine-map QTLs for diabetes[20] and fear-related behavior phenotypes.[21]

In a previous study, we demonstrated that skeletal mass, structure and biomechanical properties vary considerably in heterogeneous stock (HS) rat strains.[22] In addition, we observed strong heritability for several of these skeletal phenotypes, suggesting that the HS rat represents a unique genetic resource for dissecting the complex genetics underlying bone fragility. In a recent study, genomic sequence data was obtained on animals from each of the HS founder strains, along with genotypes for a dense SNP marker map in a large number of HS offspring. Phenotypic data for over 150 physiological and other phenotypes, including measures of bone density, were also obtained on the HS offspring, and over 1,000 genomic regions demonstrated association with one or more of the phenotypes measured.[23] The sequence data from the founder strains were then used to identify single genomic variants that fully accounted for an observed association in one of these regions, using a novel method that exploits the HS pedigree structure.[23] Numerous such variants were identified for phenotypes measured in the HS offspring; however, no single genetic variants explaining associations with bone phenotypes were detected, consistent with the complex genetic architecture of bone density observed previously both in humans and animal models.[23]

The purpose of this study is to address this genetic complexity by use of dense SNP genotype data to perform high-resolution mapping for bone mineral density (BMD) phenotypes in HS rat offspring. We hypothesize that we will detect and localize QTLs for several key BMD phenotypes at the most common skeletal fracture sites. We expect that the QTLs detected via the HS approach will comprise much smaller genomic regions than bone density QTLs detected by us and others using inbred rat crosses. In the future, these results may allow more detailed study of the smaller number of genes in the regions detected compared to prior approaches, and contribute to better understanding of the complex genetic architecture of the BMD phenotypes in HS rats.

Materials and Methods

Animals

We used 1524 HS rats (male n=728; female n=796) in this study. The HS rats were bred and grown at the Autonomous University of Barcelona. Microchips were implanted in these rats for identification and multiple physiology and behavior phenotypes were obtained at several time points. The rats were housed in cages in pairs (males) and trios (females) and maintained with food and water available ad libitum, under conditions of controlled temperature (22 + 2 °C), 50-70% relative humidity and a 12-h light-dark cycle (lights on at 0800 h). The HS rats were raised over 2.5 years in batches of approximately 250 animals in accordance with the Spanish legislation on “Protection of Animals used for Experimental and Other Scientific Purposes” and the European Communities Council Directive (86/609/EEC).

Euthanasia and specimen collection

HS rats were euthanized between 17 and 20 weeks of age by ether inhalation. The lower limbs and lumbar vertebrae (L3-5) were dissected from these animals. The lower limbs on the right side were immediately stored at −20°C for subsequent biomechanical testing. The

lower limbs on the left side were stripped of muscle, transferred to 70% ethyl alcohol and stored at 4°C for densitometry analyses.

Dual energy X-ray absorptiometry (DXA)

The left femur and lumbar vertebrae 3-5 (L3-5) of the HS rats were scanned using DXA (PIXImus II mouse densitometer; Lunar Corp., Madison, WI, USA) with ultra-high resolution (0.18 × 0.18 mm/pixel). During scanning dissected bones were positioned on a platform supplied by the manufacturer. After completion of the scan of each bone, mutually exclusive region of interest (ROI) boxes were drawn around the bone from which aBMD (g/cm^2) and BMC (g) measurements were obtained.

Peripheral quantitative computed tomography (pQCT)

The left femurs were placed in plastic tubes filled with 70% ethyl alcohol and centered in the gantry of a Norland Stratec XCT Research SA+pQCT (Stratec Electronics, Pforzheim, Germany). Single slice measurements of 0.26 mm thickness and a voxel size of 0.07 mm were taken for the femur. Two femoral cross-sectional slices were obtained for each femur: one slice through femoral midshaft and one slice approximately 1 mm below the growth plate of distal femur. The slice through the femur midshaft included only cortical bone, whereas the distal slice included the cortical shell and secondary spongiosa. L5 vertebrae were scanned in cross-section at the caudo-cranial center of the vertebral body. For femoral neck, five consecutive scans perpendicular to the neck axis were obtained 0.25 mm apart from each other starting at the base of the femoral head and ending at the greater trochanter. For each slice, the X-ray source was rotated through 180° of projection. Density thresholds of 500 and 900 were used to identify trabecular and compact bone. Volumetric density (vBMD; mg/cm^3) of cortical and trabecular bone were measured from each slice separately at distal femur and L5 spine. vBMD for femoral neck was measured from the average values of all five slices. In addition, total cross-sectional area at femur midshaft and L5 spine were measured to enable the determination of whether BMD QTLs detected were due primarily to bone size effects.

Genotyping

DNA was extracted from liver tissues from 8 original founders and 1524 HS rats using standard protocols. Genotypes for over 900,000 SNPs for each rat were obtained from an Affymetrix rat custom SNP array (www.affymetrix.com). SNPs were algorithmically selected taking into account the strain distribution pattern to maximize the information available for mapping as well as the SNP call quality metrics. The set of SNPs were pruned to approximately 70,000 high quality SNPs which covered the HS rat genome with a mean linkage disequilibrium coefficient between neighboring SNPs of 0.95.

Statistical genetic analysis

Haplotypes were constructed for each rat across the genome using the multipoint haplotype reconstruction method HAPPY (http://www.well.ox.ac.uk/happy).[19] HAPPY uses a hidden Markov model to calculate the probability of descent from each founder at each genotyped locus. A mixed model approach was then employed to test for association between each

haplotype and the bone phenotype of interest. The distinguishing feature of this model for the HS analysis is the ability to account for the complex family structure of the HS rat. Variance components to correct for pedigree relationships were estimated using the EMMA package for the R statistical software[25], and the test for association was conducted for each phenotype via a mixed model, adjusting for age, sex, body weight and batch. At each genotyped SNP on chromosomes 1-22 and X, the $-\log_{10}$(p-value) was computed. A genome-wide empiric significance threshold was obtained for each phenotype, corresponding to the 5% false discovery rate for that particular measure. A corresponding conservative overall threshold for the current study ($P<3 \times 10^{-6}$; **$-\log_{10}P=5.5$**) was obtained by taking the **largest $-\log_{10}P$ value among** these thresholds across all the bone density phenotypes. To further reduce type I error, the resample-based inclusion probability (RMIP) was computed for each QTL detected, and peaks with RMIP<0.3 (corresponding to an approximate specificity of 0.75) were excluded. All models were fitted using the statistical language R (R-Development-Core-Team 2004).[26] A 95% confidence interval for the position of each QTL detected was obtained as described previously[9,27], assuming a χ^2_1distribution for lod to $-\log_{10}$(p-value) conversion. The sample had greater than 80% power to detect QTLs contributing 5% of the total variation in the BMD phenotypes measured, and approximately 70% power for QTLs of 3% effect at the conservative FDR and RMIP significance thresholds employed.

Results

Figure 1 shows linkage results obtained throughout the genome for the measurements of femur bone mineral content and density (A-D), femur neck density (E,F), and lumbar bone mineral content and density (G-I) in this study. Several QTLs reaching the genome-wide FDR and RMIP significance thresholds were observed in the HS rat sample, and are included in Table 1. Candidate genes within the 95% confidence intervals (CI) for these QTLs are listed in Table 2.

Genome-wide significant association results for femur mineral content and density

On chromosome 10 at position 46.5 Mb, significant linkage was detected for femur BMC with a −logP value of 5.64 ($p=2.3 \times 10^{-6}$; Figure 2A and Table 1). The CI for this QTL spanned less than half a megabase (Mb). On chromosome 9, a QTL was identified which was linked to several femur density phenotypes (Figure 2B). Within this region, a QTL for distal femur vBMD was observed, with a −logP value of 5.68 ($p=2.1 \times 10^{-6}$). The same chromosome 9 region, spanning approximately 3.5 Mb, contained an additional QTL with substantial (but not genome-wide significant) evidence for linkage with distal femur trabecular vBMD ($p=1.8 \times 10^{-5}$).

Genome-wide significant association results for femur neck bone mineral density

We observed two genome-wide significant QTLs for femoral neck density phenotypes, one each for femoral neck vBMD (Figure 2B) and for femoral neck cortical vBMD (Figure 2C). In the same 3.5 Mb region of chromosome 9 that our study identified for other femur density measures, a QTL for femoral neck vBMD was observed with a significant −logP value of 5.56 ($p=2.7 \times 10^{-6}$). This coincided with the position of the distal femur and trabecular

vBMD chromosome 9 QTLs above. With femur neck cortical vBMD, a QTL was observed at 182.1 Mb on chromosome 2, with a −logP value of 5.77 ($p=1.7 \times 10^{-6}$; Figure 2C and Table 1).

Genome-wide significant association results for lumbar bone mineral content and density

An additional QTL at the proximal end of chromosome 13 was identified for lumbar 5 trabecular vBMD ($p=9.7 \times 10^{-8}$; Figure 2D and Table 1). This QTL spanned 2.5 Mb, with a −logP value of 7.01.

Discussion

In previous work, we identified QTLs for bone density phenotypes using the F2 intercross approach in the rat model.[13] While quite powerful for QTL detection, this approach often results in QTL intervals encompassing a third to half of a chromosome containing several hundred genes. In this study, we exploited the unique genetic architecture in HS rat to detect and localize QTLs in a smaller region for several key BMD phenotypes at most common skeletal fracture sites. We utilized the pedigree structure and sequence data from the founder HS strains to identify genomic variants associated with these QTLs in the HS offspring and identified several chromosomal regions with strong evidence of association with bone mineral density. Importantly, most of these loci were localized to very small genomic regions (1-3 Mb) compared to the F2 design used previously for QTL mapping. This allows us to identify **a much more** focused list of potential candidate genes under each QTL peak for future functional studies, which are often prohibitive to conduct in large number of genes. In addition to several novel genes detected in the HS rat model (*Aars2*, ***Adar,*** *Atpaf2*, ***Cdc5l, Chrnb2,*** *Cntnap5b*, ***Dap3, Dcst1/2, Kcnn3,*** *Lrrc48*, *Mrpl14*, *Nup210l*, ***Pbxip1, Pklr, Scamp3, Shc1, Spats1, Supt3h, Tcte1,*** *Tom1l2*, ***Tmem63b***, and *Ube2q1*, ***Zbtb7b***), we also identified skeletal candidate genes underlying these QTLs (***Adam15***, *Capn11*, ***Efna4***, *Il6*, *Slc39a1*, *Srebf1*, ***Thbs3, Tpm3***, ***Rai1***, *Runx2 and Vegfa*) that have been previously shown to have a role in skeletal development and homeostasis.

Among all the genes detected under the relatively narrow intervals in this study (Table 2), there are several genes in particular that have been previously reported to have important roles in bone homeostasis. **Lack of *Adam15*** in mice is associated with increased osteoblast function and bone mass.[28] The calpains are a family of calcium-dependent thiol proteases involved in intracellular protein processing and have been shown to modulate cellular proliferation and differentiation in rodent osteoblast cells.[29] Also, these proteases are required for normal osteoclast and chrondrocyte function.[30,31] ***Epha4*** is necessary during bone growth and acts as a negative regulator of osteoclast activity.[32,33] *IL-6* receptor expression is increased during *in vitro* osteoblast differentiation.[34,35] In addition, these receptors are involved in osteoclast formation and function.[36] ***Rai1*** knockout mice are growth retarded and displays malformations in both the craniofacial and the axial skeleton.[37] Runx2 is a major transcription factor for chondrocyte and osteoblast differentiation.[38] ***Thbs3*** influences geometric and biomechanical properties of bone.[39] *Vegf* is well known for its role in angiogenesis and osteogenesis[40-42], and *Tpm3* is expressed during osteoclast fusion and regulates osteoclast cytoskeletal morphology.[43] Association of a polymorphism in *Srebf1*

with osteonecrosis of the femoral head has been observed in Koreans.[44] *Slc39a1* or *Zip1* is expressed in osteoclasts and overexpression of the Zip1 induces osteogenic phenotype.[45,46]

In this study, we were able to replicate several chromosomal regions previously identified in our inbred F2 studies in HS rats. For example, we detected association with distal femur density in the HS rats on chromosome 9 (LOD 5.68), which overlapped the QTLs in our F344 X LEW and COP X DA F2 cross for femur neck structural phenotypes.[9,11] Similarly, the femoral neck cortical vBMD QTL identified in HS rats on chromosome 2 (LOD 5.77) overlapped the QTL in F344 X LEW F2 cross for the same phenotype.[11] Importantly, using HS rats, we were able to fine-map these regions to 1-3 Mb resolution, enabling us to identify a much smaller number of potential candidate genes on chromosomes 2 and 9 (Table 2). We also identified several novel chromosomal regions linked to bone density phenotypes in HS rats (Table 2) not found in our F2 studies. On chromosome 9, a QTL was identified which was linked to several femur density phenotypes (Figure 2B) including distal femur total (both cortical and trabecular) and distal femur trabecular vBMD as well as femur neck vBMD. These results indicate that same gene/s may contribute not only trabecular and cortical compartments of bone mineral density but also influence density at different skeletal sites even within a given bone. Previous studies demonstrated site-specific genetic regulation of trabecular and cortical bone density in human and rodents.[7,13,47,48] Thus, it is likely that sets of bone-specific genes might influence density across the different bones and the genetic architecture within the different combinations of these bone-specific genes might ultimately regulate the site-specific bone density.

The QTL region for femoral neck cortical vBMD on chromosome 2 in HS rat is syntenic to human 1q21.3-23.1, where linkage to spine BMD was detected previously.[49] The QTL region for distal femur and femoral neck vBMD on chromosome 9 in HS rat is homologous to the regions of mouse chromosome 17 (38.3-46.5 Mb) and human chromosome 6 **(6p12.3-21.2).** Linkage to mouse total body BMD and femur strength were reported before in this homologous region.[50,51] In addition, the human homologous region was previously linked to **femoral neck BMD** and osteoarthritis and rheumatoid arthritis QTLs.[52-54] Similarly, femur BMC QTL detected on chromosome 10 in HS rat is homologous to the mouse chromosome 11 (59.4-60.6 Mb), which was previously linked to peak BMD.[55,56] The human homologous region of 17p11.2 harbors gene that when overexpress lead to osteosarcoma.[57] Interestingly, deletion of the human syntenic region on chromosome 18q22 that corresponds to the QTL region on chromosome 13 for lumbar trabecular vBMD in HS rat was associated with multiple vertebral segmentation defects.[58]

In this study, we demonstrated that HS rats are a powerful resource for fine mapping of QTLs for bone mineral density phenotypes. The complexity of the BMD phenotype in the rat is evident due to the inability to identify any specific sequence variants in the HS founder strains that fully accounted for BMD QTLs in our recent study.[23] This suggests that the genetic variation underlying the BMD QTL is due to multiple variants inherited from different founders and may also reflect interactions among the variants. Given the results of the analysis of the founder animal sequencing data, we have now focused on the identification of additional BMD QTLs in the HS rat model using conservative genome-wide significance thresholds. For the bone density QTLs detected, this approach had the

great benefit of allowing us to delineate a much smaller chromosomal interval and thus narrower list of potential candidate than the F2 approach. We anticipate that sequencing studies in the HS offspring in these narrowed regions will be necessary to augment the founder strain sequence data currently available as part of the HS collaboration.[23] The availability of these data will allow the dissection of the complex genetic interactions among these sequence variants which likely underlies the BMD phenotypes in the tested animals.

Acknowledgments

We thank Carme Mont-Cardona for animal care and tissue harvest. This work was supported by the US National Institutes of Health through the following grants: AR047822 and AG041517. The research leading to these results has received funding from the European Union's Seventh Framework Programme (FP7/2007-2013) under grant agreement HEALTH-F4-2010-241504 (EURATRANS), the Wellcome Trust (090532/Z/09/Z, 083573/Z/07, 089269/Z/09/Z), the Ministerio de Ciencia e Innovación (reference PSI2009-10532) and the Fundació La Marató TV3 (reference 092630).

References

1. Kanis JA, Melton LJ, Christiansen C, Johnston CC, Khaltaev N. The diagnosis of osteoporosis. J Bone Miner Res. 1994; 9:1137–41. [PubMed: 7976495]
2. Cummings SR, Black DM, Nevitt MC, Browner W, Cauley J, Ensrud K, et al. The Study of Osteoporotic Fractures Research Group. Bone density at various sites for prediction of hip fractures. Lancet. 1993; 341:72–75. [PubMed: 8093403]
3. Faulkner KG, Cummings SR, Black D, Palermo L, Gluer CC, Genant HK. Simple measurement of femoral geometry predicts hip fracture: the study of osteoporotic fractures. J Bone Miner Res. 1993; 8:1211–17. [PubMed: 8256658]
4. Peacock M, Turner CH, Liu G, Manatunga AK, Timmerman L, Johnston CC Jr. Better discrimination of hip fracture using bone density, geometry and architecture. Osteoporos Int. 1995; 5:167–73. [PubMed: 7655177]
5. Arden NK, Baker J, Hogg C, Bann K, Spector TD. The heritability of bone mineral density, ultrasound of the calcaneus and hip axis length: a study of postmenopausal twins. J Bone Miner Res. 1996; 11:530–34. [PubMed: 8992884]
6. Garnero P, Arden NK, Griffiths G, Delmas PD, Spector TD. Genetic influence on bone turnover in postmenopausal twins. J Clin Endocrinol Metab. 1996; 81:140–46. [PubMed: 8550741]
7. Peacock M, Turner CH, Econs MJ, Foroud T. Genetics of osteoporosis. Endocr Rev. 2002; 23:378–83.
8. Ralston SH. Genetic determinants of osteoporosis. Curr Opin Rheumatol. 2005; 17:475–79. [PubMed: 15956846]
9. Alam I, Sun Q, Liu L, Koller DL, Carr LG, Econs MJ, et al. Sex-specific genetic loci for femoral neck bone mass and strength identified in inbred COP and DA rats. J Bone Miner Res. 2008; 23:850–59. [PubMed: 18282130]
10. Sun Q, Alam I, Liu L, Koller DL, Carr LG, Econs MJ, et al. Genetic loci affecting bone structure and strength in inbred COP and DA rats. Bone. 2008; 42:547–53. [PubMed: 18158281]
11. Alam I, Sun Q, Liu L, Koller DL, Fishburn T, Carr LG, et al. Identification of a quantitative trait locus on rat chromosome 4 that is strongly linked to femoral neck structure and strength. Bone. 2006; 39:93–99. [PubMed: 16461031]
12. Alam I, Sun Q, Liu L, Koller DL, Fishburn T, Carr LG, et al. Whole-genome scan for linkage to bone strength and structure in inbred Fischer 344 and Lewis rats. J Bone Miner Res. 2005; 20:1589–96. [PubMed: 16059631]
13. Koller DL, Alam I, Sun Q, Liu L, Fishburn T, Carr LG, et al. Genome screen for bone mineral density phenotypes in Fischer 344 and Lewis rats. Mammalian Genome. 2005; 16:578–86. [PubMed: 16180139]

14. Alam I, Sun Q, Koller DL, Liu L, Liu Y, Edenberg HJ, et al. Genes influencing spinal bone mineral density in inbred F344, LEW, COP and DA rats. Functional and Integrative Genomics. 2009; 10:63–72. [PubMed: 19841953]
15. Alam I, Sun Q, Koller DL, Liu L, Liu Y, Edenberg HJ, et al. Differentially expressed genes strongly correlated with femur strength in rats. Genomics. 2009; 94:257–62. [PubMed: 19482074]
16. Alam I, Sun Q, Liu L, Koller DL, Liu Y, Edenberg HJ, et al. Genomic expression analysis of rat chromosome 4 for skeletal traits at femoral neck. Physiological Genomics. 2008; 35:191–96. [PubMed: 18728226]
17. Hansen C, Spuhler K. Development of the National Institutes of Health genetically heterogeneous rat stock. Alcohol Clin Exp Res. 1984; 8:477–9. [PubMed: 6391259]
18. Boucher W, Cotterman CW. On the classification of regular systems of inbreeding. J Math Biol. 1990; 28:293–305. [PubMed: 2332706]
19. Mott R, Talbot CJ, Turri MG, Collins AC, Flint J. A method for fine mapping quantitative trait loci in outbred animal stocks. Proc Natl Acad Sci USA. 2000; 97:12649–54. [PubMed: 11050180]
20. Solberg Woods LC, Holl K, Tschannen M, Valdar W. Fine-mapping a locus for glucose tolerance using heterogeneous stock rats. Physiol Genomics. 2010; 41:102–8. [PubMed: 20068026]
21. Johannesson M, Lopez-Aumatell R, Stridh P, Diez M, Tuncel J, Blázquez G, et al. A resource for the simultaneous high-resolution mapping of multiple quantitative trait loci in rats: the NIH heterogeneous stock. Genome Res. 2009; 19:150–8. [PubMed: 18971309]
22. Alam I, Koller DL, Sun Q, Roeder RK, Cañete T, Blázquez G, et al. Heterogeneous stock rat: A unique animal model for mapping genes influencing bone fragility. Bone. 2011; 48:1169–1177. [PubMed: 21334473]
23. Baud A, Hermsen R, Guryev V, Stridh P, Graham D, McBride MW, et al. Combined sequence-based and genetic mapping analysis of complex traits in outbred rats. Nat Genet. 2013; 45(7):767–75. [PubMed: 23708188]
24. Yalcin B, Flint J, Mott R. Using progenitor strain information to identify quantitative trait nucleotides in outbred mice. Genetics. 2005; 171(2):673–81. [PubMed: 16085706]
25. Kang HM, Zaitlen NA, Wade CM, Kirby A, Heckerman D, Daly MJ, et al. Efficient control of population structure in model organism association mapping. Genetics. 2008; 178(3):1709–23. [PubMed: 18385116]
26. R. Development Core Team. R: A language and environment for statistical computing. R Foundation for Statistical Computing; Vienna, Austria: 2004.
27. Visscher PM, Thompson R, Haley CS. Confidence intervals in QTL mapping by bootstrapping. Genetics. 1996; 143(2):1013–20. [PubMed: 8725246]
28. Marzia M, Guaiquil V, Horne WC, Blobel CP, Baron R, Chiusaroli R. Lack of ADAM15 in mice is associated with increased osteoblast function and bone mass. Biol Chem. 2011; 392(10):877–85. [PubMed: 21801086]
29. Murray SS, Grisanti MS, Bentley GV, Kahn AJ, Urist MR, Murray EJ. The calpain-calpastatin system and cellular proliferation and differentiation in rodent osteoblastic cells. Exp Cell Res. 1997; 233(2):297–309. [PubMed: 9194492]
30. Marzia M, Chiusaroli R, Neff L, Kim NY, Chishti AH, Baron R, et al. Calpain is required for normal osteoclast function and is down-regulated by calcitonin. J Biol Chem. 2006; 281(14):9745–54. [PubMed: 16461769]
31. Kashiwagi A, Schipani E, Fein MJ, Greer PA, Shimada M. Targeted deletion of Capn4 in cells of the chondrocyte lineage impairs chondrocyte proliferation and differentiation. Mol Cell Biol. 2010; 30(11):2799–810. [PubMed: 20368361]
32. Stiffel V, Amoui M, Sheng MH, Mohan S, Lau KH. EphA4 receptor is a novel negative regulator of osteoclast activity. J Bone Miner Res. Aug 26.2013 doi: 10.1002/jbmr.2084.
33. Ting MC, Wu NL, Roybal PG, Sun J, Liu L, Yen Y, Maxson RE Jr. EphA4 as an effector of Twist1 in the guidance of osteogenic precursor cells during calvarial bone growth and in craniosynostosis. Development. 2009; 136(5):855–64. [PubMed: 19201948]
34. Li Y, Bäckesjö CM, Haldosén LA, Lindgren U. IL-6 receptor expression and IL-6 effects change during osteoblast differentiation. Cytokine. 2008; 43(2):165–73. [PubMed: 18555695]

35. Liu F, Aubin JE, Malaval L. Expression of leukemia inhibitory factor (LIF)/interleukin-6 family cytokines and receptors during in vitro osteogenesis: differential regulation by dexamethasone and LIF. Bone. 2002; 31(1):212–9. [PubMed: 12110437]
36. Palmqvist P, Persson E, Conaway HH, Lerner UH. IL-6, leukemia inhibitory factor, and oncostatin M stimulate bone resorption and regulate the expression of receptor activator of NF-kappa B ligand, osteoprotegerin, and receptor activator of NF-kappa B in mouse calvariae. J Immunol. 2002; 169(6):3353–62. [PubMed: 12218157]
37. Bi W, Ohyama T, Nakamura H, Yan J, Visvanathan J, Justice MJ, Lupski JR. Inactivation of Rai1 in mice recapitulates phenotypes observed in chromosome engineered mouse models for Smith-Magenis syndrome. Hum Mol Genet. 2005; 14(8):983–95. [PubMed: 15746153]
38. Karsenty G. Transcriptional control of skeletogenesis. Annu Rev Genomics Hum Genet. 2008; 9:183–96. [PubMed: 18767962]
39. Hankenson KD, Hormuzdi SG, Meganck JA, Bornstein P. Mice with a disruption of the thrombospondin 3 gene differ in geometric and biomechanical properties of bone and have accelerated development of the femoral head. Mol Cell Biol. 2005; 25(13):5599–606. [PubMed: 15964815]
40. Mayer H, Bertram H, Lindenmaier W, Korff T, Weber H, Weich H. Vascular endothelial growth factor (VEGF-A) expression in human mesenchymal stem cells: autocrine and paracrine role on osteoblastic and endothelial differentiation. J Cell Biochem. 2005; 95(4):827–39. [PubMed: 15838884]
41. Zelzer E, Mamluk R, Ferrara N, Johnson RS, Schipani E, Olsen BR. VEGFA is necessary for chondrocyte survival during bone development. Development. 2004; 131(9):2161–71. [PubMed: 15073147]
42. Behr B, Tang C, Germann G, Longaker MT, Quarto N. Locally applied VEGFA increases the osteogenic healing capacity of human adipose derived stem cells by promoting osteogenic and endothelial differentiation. Stem Cells. 2011; 29(2):286–96. [PubMed: 21732486]
43. McMichael BK, Kotadiya P, Singh T, Holliday LS, Lee BS. Tropomyosin isoforms localize to distinct microfilament populations in osteoclasts. Bone. 2006; 39(4):694–705. [PubMed: 16765662]
44. Lee HJ, Choi SJ, Hong JM, Lee WK, Baek JI, Kim SY, et al. Association of a polymorphism in the intron 7 of the SREBF1 gene with osteonecrosis of the femoral head in Koreans. Ann Hum Genet. 2009; 73(1):34–41. [PubMed: 19040658]
45. Khadeer MA, Sahu SN, Bai G, Abdulla S, Gupta A. Expression of the zinc transporter ZIP1 in osteoclasts. Bone. 2005; 37(3):296–304. [PubMed: 16005272]
46. Tang Z, Sahu SN, Khadeer MA, Bai G, Franklin RB, Gupta A. Overexpression of the ZIP1 zinc transporter induces an osteogenic phenotype in mesenchymal stem cells. Bone. 2006; 38(2):181–98. [PubMed: 16203195]
47. Duncan EL, Cardon LR, Sinsheimer JS, Wass JA, Brown MA. Site and gender specificity of inheritance of bone mineral density. J Bone Miner Res. 2003; 18:1531–1538. [PubMed: 12929944]
48. Ioannidis JP, Ng MY, Sham PC, Zintzaras E, Lewis CM, Deng HW, et al. Meta-analysis of genome-wide scans provides evidence for sex- and site-specific regulation of bone mass. J Bone Miner Res. 2007; 22(2):173–83. [PubMed: 17228994]
49. Koller DL, Econs MJ, Morin PA, Christian JC, Hui SL, Parry P, et al. Genome screen for QTLs contributing to normal variation in bone mineral density and osteoporosis. J Clin Endocrinol Metab. 2000; 85(9):3116–20. [PubMed: 10999795]
50. Li X, Masinde G, Gu W, Wergedal J, Mohan S, Baylink DJ. Genetic dissection of femur breaking strength in a large population (MRL/MpJ × SJL/J) of F2 Mice: single QTL effects, epistasis, and pleiotropy. Genomics. 2002; 79(5):734–40. [PubMed: 11991724]
51. Masinde GL, Li X, Gu W, Wergedal J, Mohan S, Baylink DJ. Quantitative trait loci for bone density in mice: the genes determining total skeletal density and femur density show little overlap in F2 mice. Calcif Tissue Int. 2002; 71(5):421–8. [PubMed: 12202954]

52. Karasik D, Myers RH, Cupples LA, Hannan MT, Gagnon DR, Herbert A, et al. Genome screen for quantitative trait loci contributing to normal variation in bone mineral density: the Framingham Study. J Bone Miner Res. 2002; 17(9):1718–27. [PubMed: 12211443]

53. Loughlin J, Mustafa Z, Irven C, Smith A, Carr AJ, Sykes B, et al. Stratification analysis of an osteoarthritis genome screen-suggestive linkage to chromosomes 4, 6, and 16. Am J Hum Genet. 1999; 65(6):1795–8. [PubMed: 10577938]

54. Jawaheer D, Seldin MF, Amos CI, Chen WV, Shigeta R, Monteiro J, et al. A genomewide screen in multiplex rheumatoid arthritis families suggests genetic overlap with other autoimmune diseases. Am J Hum Genet. 2001; 68(4):927–36. [PubMed: 11254450]

55. Klein RF. Genetic regulation of bone mineral density in mice. J Musculoskelet Neuronal Interact. 2002; 2(3):232–6. [PubMed: 15758441]

56. Beamer WG, Shultz KL, Donahue LR, Churchill GA, Sen S, Wergedal JR, et al. Quantitative trait loci for femoral and lumbar vertebral bone mineral density in C57BL/6J and C3H/HeJ inbred strains of mice. J Bone Miner Res. 2001; 16(7):1195–206. [PubMed: 11450694]

57. van Dartel M, Hulsebos TJ. Amplification and overexpression of genes in 17p11.2 ~ p12 in osteosarcoma. Cancer Genet Cytogenet. 2004; 153(1):77–80. [PubMed: 15325100]

58. Dowton SB, Hing AV, Sheen-Kaniecki V, Watson MS. Chromosome 18q22.2-->qter deletion and a congenital anomaly syndrome with multiple vertebral segmentation defects. J Med Genet. 1997; 34(5):414–7. [PubMed: 9152840]

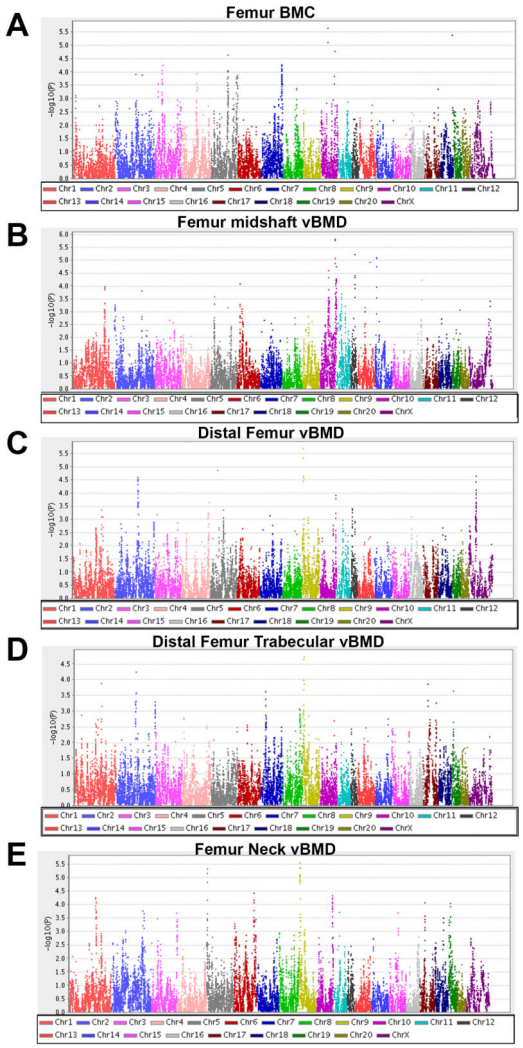

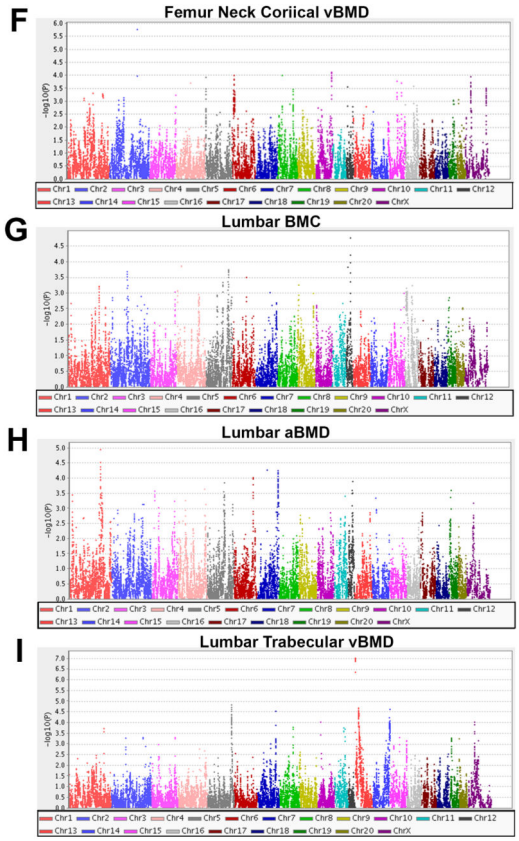

Fig. 1.

Genome-wide plots for femur BMC (A), femur midshaft vBMD (B), distal femur vBMD (C), distal femur trabecular vBMD (D), femoral neck vBMD (E), femoral neck cortical vBMD (F), lumbar BMC (G), lumbar aBMD (H) and lumbar 5 trabecular vBMD (I). The −log10P values plotted on the Y-axis versus chromosome position on the X-axis. For comparability with other mapping studies, QTL results are shown at each position regardless of the conservative RMIP threshold (0.3) employed to select the most robust QTLs for our report.

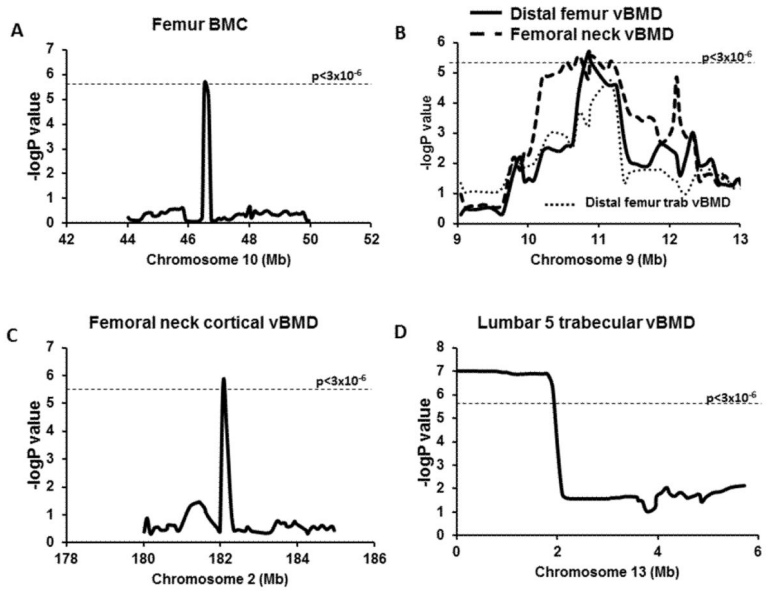

Fig. 2.

Association results for femur BMC on chromosome 10 (A), distal femur vBMD, distal femur trab vBMD and femoral neck vBMD on chromosome 9 (B), femoral neck cortical vBMD on chromosome 2 (C) and lumbar 5 trabecular vBMD on chromosome 13 (D). The −logP values are plotted on the Y-axis vs. the chromosomal position (MB) on the X-axis. The dashed horizontal lines indicate the threshold value for genome-wide significance corresponding to FDR=5% ($p<3 \times 10^{-6}$).

Table 1

Chromosomal regions associated with significant linkage ($p<3 \times 10^{-6}$) for bone mineral density phenotypes

Phenotypes	Chromosome	Position (bp)	Interval (Mb)	p-value	Male $\log_{10}$P value	Female $\log_{10}$P value	Combined $\log_{10}$P value
Femoral neck cortical vBMD (mg/cm^3)	2	182070708	180.9 - 182.3	1.71E-06	4.17	1.19	5.77
Distal femur vBMD (mg/cm^3)	9	10852281	9.6 - 13.1	2.07E-06	1.99	3.4	5.68
Femoral neck vBMD (mg/cm^3)	9	10723437	9.6 - 13.1	2.73E-06	1.85	4.27	5.56
Femur BMC (g)	10	46530592	46.3 - 46.8	2.27E-06	3.76	0.72	5.64
Lumbar 5 trabecular vBMD (mg/cm^3)	13	130318	0 - 2.5	9.74E-08	5.4	0.1	7.01

Table 2

Candidate genes within the chromosomal locations with significant ($p<3 \times 10^{-6}$) associations for bone mineral density phenotypes

Phenotypes	Chromosome	Interval (Mb)	Gene symbol	Gene name	Human synteny
Femoral neck cortical vBMD (mg/cm^3)	2	180.9 - 182.3	*Ube2q1*	Ubiquitin-conjugating enzyme E2 Q1	**1q21.3 - 1q23.1**
			Il6ra	Interleukin-6 receptor subunit alpha	
			Tpm3	Tropomyosin alpha-3 chain	
			Nup210l	Nuclear pore membrane glycoprotein 210-like	
			Slc39a1	Zinc transporter ZIP1	
			Dap3	**Death associated protein 3**	
			Pklr	**Pyruvate kinase liver and RBC**	
			Scamp3	**Secretory carrier membrane protein 3**	
			Thbs3	**Thrombospondin 3**	
			Efna1/3/4	**Ephrin A1/3/4**	
			Dcst1/2	**DC-STAMP domain containing 1/2**	
			Shc1	**SHC (Src homology 2 domain containing) transforming protein 1**	
			Adam15	**ADAM metallopeptidase domain 15**	
			Zbtb7b	**Zinc finger and BTB domain containing 7B**	
			Pbxipl	**Pre-B-cell leukemia homeobox interacting protein 1**	
			Kcnn3	**Potassium intermediate/small conductance calcium-activated channel subfamily N member 3**	
			Adar	**Adenosine deaminase RNA-specific**	
			Chrnb2	**Cholinergic receptor nicotinic beta 2 (neuronal)**	
Distal femur vBMD (mg/cm^3)	9	9.6 - 13.1	*Vegfa*	Vascular endothelial growth factor A	**6p12.3-21.2**
Femoral neck vBMD (mg/cm^3)	9	9.6 - 13.1	*Runx2*	Runt related transcription factor 2	
			Aars2	Probable alanyl-tRNA synthetase, mitochondrial	
			Mrpl14	39S ribosomal protein L14, mitochondrial	
			Capn11	Calpain 11	
			Tmem63b	**Transmembrane protein 63B**	
			Tmem151b	**Transmembrane protein 151B**	
			Tctel	**T-complex-associated testis expressed 1**	
			Cdc5l	**Cell division cycle 5-like**	

Phenotypes	Chromosome	Interval (Mb)	Gene symbol	Gene name	Human synteny
			Supt3h	**Suppressor of Ty3 homolog (S. cerevisiae)**	
			Spats1	**Spermatogenesis associated serine-rich 1**	
			Hsp90ab1	**Heat shock protein 90 alpha (cytosolic) class B member 1**	
Femur BMC (g)	10	46.3 - 46.8	*Srebf1*	Sterol regulatory element-binding protein 1	**17p11.2**
			Tom1l2	TOM1-like protein 2	
			Lrrc48	Leucine-rich repeat-containing protein 48	
			Atpaf2	ATP synthase mitochondrial F1 complex assembly factor 2	
			Rail	**Retinoic acid induced 1**	
Lumbar 5 trabecular vBMD (mg/cm^3)	13	0 - 2.5	*Cntnap5b*	Contactin-associated protein like 5-2	**2q14.3**
			SNORA17	Small nucleolar RNA SNORA17	18q22.1
			7SK	7SK RNA	